Available online at www.sciencedirect.com
ScienceDirect
Earth and Planetary Science Letters 265 (2008) 666–671
EPSL
www.elsevier.com/locate/epsl

Relation between neighbouring grains in the upper part of the *NorthGRIP* ice core — Implications for rotation recrystallization

G. Durand [a,*], A. Persson [a], D. Samyn [b], A. Svensson [a]

[a] *Niels Bohr Institute, Ice and Climate Group, University of Copenhagen, Denmark*
[b] *Université Libre de Bruxelles, Laboratoire de Glaciologie, Belgium*

Received 7 May 2007; received in revised form 30 October 2007; accepted 4 November 2007
Available online 12 November 2007
Editor: G.D. Price

Abstract

We propose a new method to investigate the relationships between neighbouring crystals and apply it to the textures measured along the upper 900 m of the *NorthGRIP* ice core. This method shows unexpected correlations between neighbours in the so-called *normal grain growth* regime, questioning the classical view on the onset of *rotation recrystallization* in ice-sheets. Moreover, the fractionation rate associated to the *rotation recrystallization* appears constant through time. Finally, grains with low-angle boundaries do not present a special distribution pattern of their *c*-axes. This suggests that *rotation recrystallization* is an isotropic process not affected by the direction of the macroscopic strain.

Keywords: ice-sheet; polycrystalline; ice recrystallization

1. Introduction

Ice cores provide a unique set of records describing changes both in past climate and atmospheric composition (EPICA Community members, 2004; North Greenland Ice Core Project members, 2004). The establishment of a depth–age relation is required for correct climatic interpretation. The most straightforward method consist in counting of annual layers along the core (Vinther et al., 2006). However, if annual layers are not resolvable, flow models are then needed. As a matter of course, understanding the deformation of natural ice is of primary importance.

Owing to the outstanding anisotropy of the ice crystal (Duval et al., 1983), *c*-axes rotate during deformation toward compressional axes and away from tensional axes (Azuma and Higashi, 1985). Thus, fabric (*c*-axes distribution) in polar ice provides a record of deformational history. Moreover the development of fabric and the strong anisotropy of the ice crystal confer to the polycrystalline ice a strain-induced anisotropy which affects the flow of ice (Mangeney et al., 1997). Fabric evolution and the induced anisotropy are now taken into account in local flow models (Gillet-Chaulet et al., 2006).

Fabric interpretation is further complicated by recrystallization processes. Three different processes

* Corresponding author.
E-mail address: gd@gfy.ku.dk (G. Durand).

0012-821X/$ - see front matter © 2007 Elsevier B.V. All rights reserved.
doi:10.1016/j.epsl.2007.11.002

are believed to occur in natural ice-sheets (Alley, 1992), following the terminology of Poirier (1985):

(i) *normal grain growth* is driven by the decrease in the grain boundary free energy. This process affects the microstructure (*i.e.*, grain boundary network) causing the mean crystal size to increase. As predicted theoretically (Alley et al., 1986), a linear increase of the mean grain area $\langle A \rangle$ is observed in the upper layers of ice-sheets for several sites in Greenland and Antarctica (Svensson et al., 2003b; Durand et al., 2006b) (see also Fig. 1). It is assumed that normal grain growth does not significantly affect the fabric evolution (Alley, 1992).

(ii) *rotation recrystallization* is the formation of new grains due to grain subdivision. Owing to the heterogeneous deformation within a grain, the grain can become bent or twisted. Dislocations tend to organize and group into walls to form sub-boundaries (*polygonization*). Misorientation between sub-grains then increases and the boundary becomes a full grain boundary, *i.e.* initial grain has been split into new grains. The onset of *rotation recrystallization* around 400 m is invoked to explain the steady grain size profile observed below this depth along the *NorthGRIP* ice core (see also Fig. 1, Svensson et al., 2003b). Such behaviour is observed at many different drilling sites (Alley, 1992). The formation of new grains associated with *rotation recrystallization* is supposed to slow down the fabric development under uniaxial compression (Castelnau et al., 1996). Moreover, the splitting of grains increases the number of neighbouring grains with a small angle of misorientation (Alley et al., 1995).

(iii) *migration recrystallization* is the rapid migration of grain boundaries between dislocation-free nuclei and deformed grains. Migration recrystallization is observed for the deepest part of ice-sheets, where temperature is higher than −10 °C and strongly affects textures (*i.e.*, microstructure and fabric) (Thorsteinsson et al., 1997). The new coarse and interlocking grains usually form in energetically favoured orientations: approximately 45° from compressional axes (Kamb, 1959). The fabric is then no more strain-induced but dictated by the stress (Duval and Castelnau, 1995).

Few studies have proposed to investigate the misorientation between neighbouring grains to improve our knowledge of recrystallization processes in ice-sheets (Alley et al., 1995; Azuma et al., 2000; Wilen et al., 2003). Here we use the recently introduced notion of texture to enlarge the description of the correlation between neighbouring grains (Durand et al., 2006a). First, a short description of the grain boundary characterization is presented in Section 2. Some applications along the upper 900 m of the *NorthGRIP* ice core are described and their implications for our knowledge of the rotation recrystallization are discussed in Section 3. Finally, Section 4 concludes.

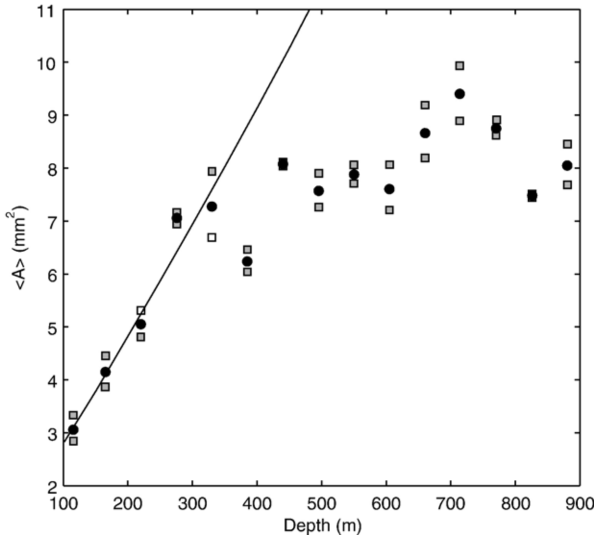

Fig. 1. Mean grain area $\langle A \rangle$ evolution along the upper 900 m of the *NorthGRIP* ice core. $\langle A \rangle$ is calculated for each 10×10 cm^2 section (squares) or for the average over two consecutive samples (filled circles) in order to smooth seasonal variability (Svensson et al., 2003a). Gray squares point out textures which present a significant over-representation of $l_{0<\theta<10}$ (see Section 3.1 and Fig. 2 for details). Black solid line indicates linear growth in the first hundredths of meters.

2. Characterization of grain boundaries

According to Poirier (1985), a grain boundary (GB) is defined as a *two dimensional lattice defect that introduces a misorientation in the lattice with no long-range stress field*. Therefore, a GB is fully described by a rotation tensor which allows to rotate one lattice to coincide with the neighbouring one, the orientation of the boundary itself with respect to one of the grains and the position of the two dimensional defect within the polycrystal. It can be convenient to distinguish between low-angle and high-angle GBs as it allows to distinguish between sub-grains and grains. Note however that distinction between low-angle and high-angle GBs is somehow arbitrary and a conventional limit of 10° to 15° misorientation angle is usually taken Poirier (1985).

Polycrystalline ice is often analyzed by preparing 2D thin sections and enlighting them under cross-polarized light. Due to the birefringence of the ice crystal, the $\boldsymbol{c}^i$ axis of a grain i can be determined. One should note that, due to the method, the lattice orientation cannot be completely determined since the crystallographic $\boldsymbol{a}^i$ axis of a grain i cannot be revealed. Moreover, topological information come from a 2D sections of a 3D material. As a result, a given GB can only be characterized by:

(i) the rotation tensor which allows to rotate $\boldsymbol{c}^i$ to $\boldsymbol{c}^j$ of nearest-neighbouring grains i and j,
(ii) the c-axis orientation of one of the adjacent grains,
(iii) the coordinates of the 1D intercept between the actual 2D GB and the plane of the section.

Most studies on the evolution of the polycrystal along ice cores used the cross-polarizers method (among others, Duval and Lorius, 1980; Lipenkov et al., 1989; Thorsteinsson et al., 1997; Durand et al., 2006b). However, for practical reasons (most of the measurements were made manually so far), these studies usually focused on the fabric and/or the topological arrangement of grains but without a link from one to the other. Only pioneering researchers have investigated the correlation of c-axes between nearest-neighbouring grains i and j by looked at the angles of misorientation θ_{ij} (Alley et al., 1995), or looked at the neighbouring interactions in fabric development model (Thorsteinsson, 2002). Note that they did not use all the information available.

Thanks to the Automatic Ice Texture Analyzers (AITA) recently developed (Wang and Azuma, 1999; Russel-Head and Wilson, 2001;Wilen et al., 2003), it is now easy to measure the full texture of a thin section: the grain boundaries network is determined and the c-axis of each grain is associated (Durand et al., 2006a). Thus, all the GB in the sections can be characterized through (i), (ii) and (iii) as defined above. In what follows, we will mostly focus on a few parameters defined as follows: θ_{ij} the misorientation angle between $\boldsymbol{c}^i$ to $\boldsymbol{c}^j$, l_{ij} the relative length of one GB with respect to the total length of GB network, $l_{0<\theta<10}$ the relative length of all low-angle GBs and $P_{0<\theta<10}$ the relative population of low-angle GBs, where a limit of 10° is taken.

In the light of this improved GB characterization, we re-analyzed the textures previously processed along the *NorthGRIP* ice core (Svensson et al., 2003b). The dataset is composed of 30 textures of 10×10 cm^2, built from 15 vertical samples 20 cm-long and 10 cm-wide taken between 115 and 882 m depth. Between these two depths, the number of grains for a given sample spans from 4560 to 1413. The present-day mean-annual layer thickness is 19.5 cm, so that the average on two consecutive textures will smooth seasonal variations (Svensson et al., 2003a).

3. Results and discussion

3.1. Preferential misorientation angle between neighbouring grains

Alley et al. (1995) have proposed to investigate the distribution of θ_{ij} between all the neighbouring grains i and j. Indeed, differences between this distribution and that of misorientation angles between randomly chosen pairs of grains (relations between neighbours are lost) can reveal some physical processes. Details on the statistical methods they used can be found in the original publication. Alley et al. (1995) applied their method to a few sections sampled from the Byrd Station (West Antarctica) ice core and showed the over-representation of low values of θ_{ij} for samples below 400 m. They attributed this effect to the onset of rotation recrystallization.

Here, we proceed to a similar type of test. First, we calculated θ_{ij} as well as the relative length l_{ij} of each GB, which allowed us to compute the distribution of the relative length l as a function of the misorientation angle θ. Such type of distribution will be referred to as D_{correl}. In Fig. 2, D_{correl} calculated for a texture sampled at 115.5 m depth is plotted with a thick solid line. Note that we have preferred to consider the relative length of GBs rather than their relative population, as the energy associated to a GB is proportional to its length (Petrenko and Whitworth, 1999). However, similar results are obtained if the distribution of the relative population versus θ is calculated. Secondly, for each grain within the microstructure, a new orientation chosen among the orientations present in the fabric is randomly assigned: the fabric is reshuffled (θ_{ij} is modified) and the microstructure is unchanged (l_{ij} is not affected). A distribution of θ versus l can be calculated for this uncorrelated texture, which is further denoted D_{uncorrel}. This procedure is repeated 200 times leading to the calculation of 200 different D_{uncorrel} sets. For a given θ bin (10°), we checked that values of the relative length $l_{\theta_1<\theta<\theta_1+10}$ computed from the 200 D_{uncorrel} curves is well fitted by a normal distribution (unpublished data). Then a 3σ probability-density envelope around the mean value calculated from the 200 D_{uncorrel} can be easily established as illustrated in Fig. 2.

It is shown in Fig. 2 that D_{uncorrel} basically follows a trend similar to that of D_{correl} for the sample considered. However, a significant over-representation $l_{0<\theta<10}$

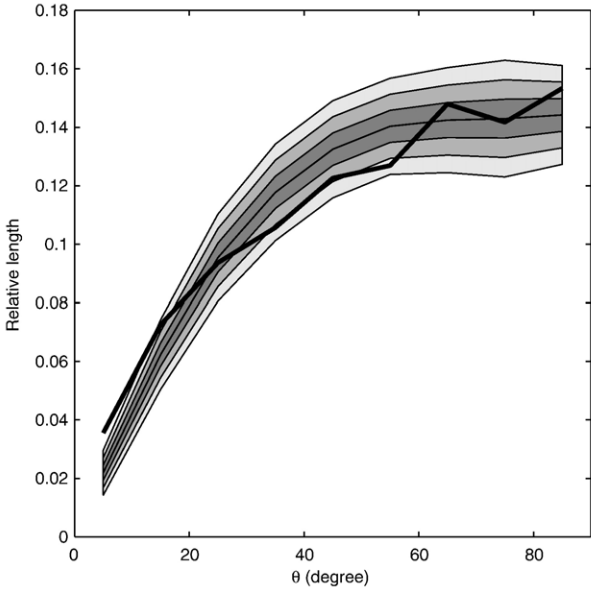

Fig. 2. Distribution of the relative length of GBs as a function of the misorientation angle θ for the texture sampled at 115.5 m. D_{correl} (see text) is plotted with a dark solid line. Gray tones correspond to 1, 2 and 3σ deviations estimated from 200 $D_{uncorrel}$s (see text). All the distributions are computed with 10° bins.

(larger than 3σ) as compared to the uncorrelated textures is evident. This method has been applied for all the 30 textures and similar results appears for most of them as pointed out by gray squares in Fig. 1. Such systematic deviations from uncorrelated textures cannot be explained by variability of the measurements; a physical process has thus to be involved. *Rotation recrystallization* is a natural candidate for an over-representation of low-angle GBs (Alley et al., 1995). However, if this effect is attributed to *rotation recrystallization*, the result suggests that this process is already active in the uppermost part of the ice-sheet, which is in opposition to the classical view.

3.2. Evolution of the relative population of low-angle grain boundaries

If *rotation recrystallization* is already occurring in the shallowest part of the *NorthGRIP* ice core, it would be interesting to estimate the evolution of its efficiency as a function of depth. Such estimation can be done through the evolution of $P_{0<\theta<10}$. Indeed, if the splitting rate increases, a larger number of low-angle boundaries is expected. Fig. 3 presents the evolution of $P_{0<\theta<10}$, as a function of age (Vinther et al., 2006), calculated for two consecutive textures. $P_{0<\theta<10}$ steadily increases with time and a linear regression gives a correlation coefficient $r=0.95$. In a steady regime (*i.e.*, all the layers have followed the same deformation and thermal history), the derivative of $P_{0<\theta<10}$ could be assimilate to a fractionation rate f of grains. As $P_{0<\theta<10}$ evolves linearly, f remains constant with time. A previous work from Mathiesen et al. (2004) has demonstrated than the competition between normal grain growth and rotation recrystallization leads to a linear increase of the grain size before reaching a constant mean grain size. Here we demonstrate that rotation recrystallization is occurring whatever the depth, even in the shallow part of the ice-sheet. The combination of this two conclusions leads us to argue that there is no need for a sudden onset of this process to explain the change in the trend of mean grain size.

It has to be mentioned, however, that the fabric is clustering with increasing depth, which also causes $P_{0<\theta<10}$ to increases with depth. For instance, an extremely marked single maximum fabric formed by grain rotation due to strain would display most $\theta_{ij}<10°$ whatever the considered GB. In order to estimate the effect of the fabric clustering on the estimation of $P_{0<\theta<10}$, a reshuffling procedure similar to the one presented in Section 3.1 is computed. For each sample, $P_{0<\theta<10}$ is calculated for 200 reshuffled fabrics leading to the estimation of the mean value $\langle P_{0<\theta<10}\rangle_{uncorrel}$ and the corresponding standard deviation. Then a 3σ probability-density envelope around $\langle P_{0<\theta<10}\rangle_{uncorrel}$ has been plotted in Fig. 3. Due to the fabric clustering with depth, $\langle P_{0<\theta<10}\rangle_{uncorrel}$ is slightly increasing. However, for all the samples $P_{0<\theta<10} \gg \langle P_{0<\theta<10}\rangle_{uncorrel}$ confirming the relevance

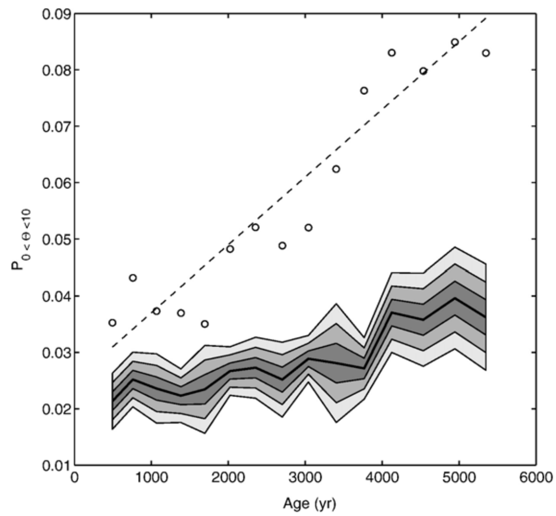

Fig. 3. Evolution of the relative population of low-angle grain boundaries ($\theta<10°$).

of our measurements in the present case. A similar approach would be meaningless for deeper samples as the contribution of *c*-axes rotation cannot be neglected anymore.

3.3. Crystallographic orientation of sub-grains

Thanks to the systematic characterization of GBs, we can also test the following hypotheses: (1) rotation recrystallization affects grains with a particular orientation, (2) rotation recrystallization affects grains independently of their orientation.

For each grain, the orientation of $\boldsymbol{c}^i$ is defined by two angles in the horizontal reference frame: the co-latitude $\theta_i^h \in [0,\pi/2]$ and the longitude $\phi_i^h \in [0, 2\pi]$. Then, θ_i^h is simply the angle between the in-situ vertical and $\boldsymbol{c}^i$. As fabrics are close to a single maximum for the upper part of the *NorthGRIP* core (Svensson et al., 2003b), a given fabric can be well described by the distribution of the number of grains belonging to a given θ_i^h bin. Such distributions with 5° bins are presented in Fig. 4 for textures sampled at 115.5 (a) and 880.5 m (b). First, one can note that *c*-axes are more clustered toward the in-situ vertical for the deepest sample as the relative number of grains presenting a large θ_i^h is decreasing to the benefit of small values of θ_i^h. This is in full agreement with the previous observations (Svensson et al., 2003b). For the same textures, same kind of distributions for the low-angle GB (grains with at least a GB presenting $\theta_{ij} < 10°$) are also plotted in Fig. 4. Using the reshuffling procedure, a 3σ variability envelope is shown as well. This shows, for both samples, a significant over-estimation of the number of low-angle GBs whatever the value of θ_i^h. Moreover, the average distribution calculated on the 200 reshuffled distributions corresponds to the mean distribution of low-angles GBs induced by grain rotation due to strain (uncorrelated low-angle GBs). The difference between the number of uncorrelated low-angles GBs and the number of measured low-angles GBs gives an estimation of the number of expected sub-grains *i.e.*, the number of sub-grains produced by *rotation recrystallization*. Then, for each θ_i^h bin, the relative number of expected sub-grains can be calculated. This has been plotted in Fig. 4(c) and (d) for the textures sampled at 115.5 and 880.5 m respectively. These distributions do not show any clear trend *i.e.*, the relative number of sub-grains produced by *rotation recrystallization* is similar whatever the value of the co-latitude. *Rotation recrystallization* is then an isotropic process and the direction of the macroscopic strain does not lead to a preferential direction of splitting.

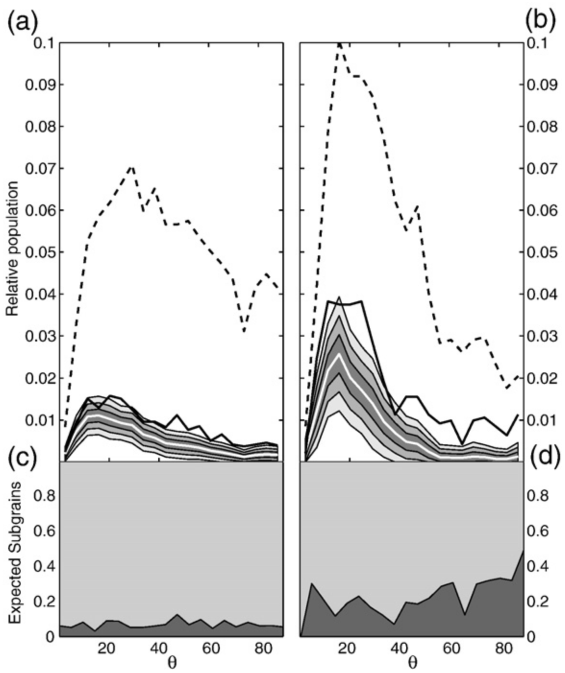

Fig. 4. Relative population as a function of the co-latitude angle for the grains (thick dashed line), low-angle GBs (thick black line) and low-angle GBs of the reshuffled texture (white line) with the corresponding confidence envelope. These distributions have been calculated for the textures sampled at 115.5 m (a) and 880.5 m (b). Relative number of expected sub-grains (see text for details) as a function of the co-latitude for the textures sampled at 115.5 m (c) and 880.5 m (d).

4. Conclusion

Thanks to more accurate measurements and a stricter definition of GBs, we have re-analyzed the upper part of the *NorthGRIP* ice core and investigated the effect of *rotation recrystallization* on the texture. The results of our work shows that *rotation recrystallization* already occurs in the upper part of the ice-sheet in the *NorthGRIP* vicinity. Moreover, the fractionation rate associated with *rotation recrystallization* appears to be constant. These experimental results are in contradiction with some deformations models that argue for the onset of *rotation recrystallization* below approximately 500 m (Montagnat and Duval, 2000). Such deformation models, which use mean values at a macroscopic scale (like the mean grain size, or the macroscopic strain rate) to estimate dislocation density and then the effect of *rotation recrystallization*, give only a crude representation of the reality as far as deformation at the grain-scale is concerned. Note also that the onset of *rotation recrystallization* is not needed to explain the change from a constant grain size increase to steady mean grain size evolution (see Fig. 1). Indeed, Mathiesen et al.

(2004) showed that a combination of grain growth and a constant fractionation rate can explain such a change in the mean grain size regime as observed along *NorthGRIP*.

Finally, we have shown that *rotation recrystallization* acts evenly whatever the orientation of the grains along the *NorthGRIP* ice core. Thus, the macroscopic direction of the strain does not affect the direction of the fractionation induced by *rotation recrystallization*.

References

Alley, R.B., 1992. Flow-law hypotheses for ice-sheet modeling. J. Glaciol. 38 (129), 245–256.

Alley, R.B., Perepezko, J.H., Bentley, C.R., 1986. Grain growth in polar ice: I. Theory. J. Glaciol. 32 (112), 415–424.

Alley, R.B., Gow, A.J., Meese, D.A., 1995. Mapping *c*-axis fabrics to study physical processes in ice. J. Glaciol. 41 (137), 197–203.

Azuma, N., Higashi, A., 1985. Formation processes of ice fabric pattern in ice sheets. Ann. Glaciol. 6, 130–134.

Azuma, N., Wang, Y., Yoshida, Y., Narita, H., Hondoh, T., Shoji, H., Watanabe, O., 2000. Crystallographic analysis of the Dome Fuji ice core. In: Hondoh, T. (Ed.), Physics of Ice Records. Hokkaido University Press, Sapporo.

Castelnau, O., Thorsteinsson, T., Kipfstuhl, J., Duval, P., Canova, G.R., 1996. Modelling fabric development along the GRIP ice core, central Greenland. Ann. Glaciol. 23, 194–201.

Durand, G., Gagliardini, O., Throsteinsson, T., Svensson, A., Kipfstuhl, J., Dahl-Jensen, D., 2006a. Ice microstructure and fabric: an up to date approach for measuring textures. J. Glaciol. 52 (179), 619–630.

Durand, G., Weiss, J., Lipenkov, V., Barnola, J.M., Krinner, G., Parrenin, F., Delmonte, B., Ritz, C., Duval, P., Roethsliberger, R., Bigler, M., 2006b. Effect of impurities on grain growth in cold ice sheets. J. Geophys. Res. 111 (F01015).

Duval, P., Lorius, C., 1980. Crystal size and climatic record down to the last ice age from Antarctic ice. Earth Planet. Sci. Lett. 48, 59–64.

Duval, P., Castelnau, O., 1995. Dynamic recrystallization of ice in polar ice sheets. J. Phys. 5 (C3), 197–205.

Duval, P., Ashby, M.F., Anderman, I., 1983. Rate controlling processes in the creep of polycrystalline ice. J. Phys. Chem. 87, 4066–4074.

EPICA Community members, 2004. Eight glacial cycles from an Antarctic ice core. Nature 429, 623–628.

Gillet-Chaulet, F., Gagliardini, O., Meyssonnier, J., Zwinger, T., Ruokolainen, J., 2006. Flow-induced anisotropy in polar ice and related ice-sheet flow modelling. J. Non-Newton. Fluid Mech. 134 (1-3), 33–43.

Kamb, W.B., 1959. Ice petrofabric observations from Blue Glacier, Washington, in relation to theory and experiment. J. Geophys. Res. 64 (11), 1891–1909.

Lipenkov, V.Y., Barov, N.I., Duval, P., Pimienta, P., 1989. Crystalline texture of the 2083 m ice core at Vostok station, antarctica. J. Glaciol. 35 (121), 392–398.

Mangeney, A., Califano, F., Hutter, K., 1997. A numerical study of anisotropic, low Reynolds number, free surface flow of ice sheet modeling. J. Geophys. Res. 102 (B10), 22,749–22,764.

Mathiesen, J., Ferkinghoff-Borg, J., Jensen, M.H., Levinsen, M., Olesen, P., Dahl-Jensen, D., Svensson, A., 2004. Dynamics of crystal formation in the Greenland NorthGRIP ice core. J. Glaciol. 50 (170), 325–328.

Montagnat, M., Duval, P., 2000. Rate controlling process in the creep of polar ice, influence of grain boundary migration associated with recrystallization. Earth Planet. Sci. Lett. 183, 179–186.

North Greenland Ice Core Project members, 2004. High resolution record of northern hemisphere climate extending into the last interglacial period. Nature 431, 147–151.

Petrenko, V.F., Whitworth, R.W., 1999. Physics of Ice. Oxford University Press.

Poirier, J.P., 1985. Creep of Crystals. Cambridge University Press.

Russel-Head, D.S., Wilson, C.J.L., 2001. Automated fabric analyser system for quartz and ice. Geol. Soc. Aust. Abstr. 64, 159.

Svensson, A., Baadsager, P., Persson, A., Hvidberg, C.S., Siggaard-andersen, M.L., 2003a. Seasonal variability in ice crystal properties at NorthGRIP: a case study around 301 m depth. Ann. Glaciol. 37, 119–122.

Svensson, A., Schmidt, K.G., Dahl-Jensen, D., Johnsen, S.J., Wang, Y., Kipfstuhl, J., Thorsteinsson, T., 2003b. Properties of ice crystals in NorthGRIP late- to middle-Holocene ice. Ann. Glaciol. 37, 113–118.

Thorsteinsson, T., 2002. Fabric development with nearest-neighbor interaction and dynamic recrystallization. J. Geophys. Res. 107 (B1), 2014.

Thorsteinsson, T., Kipfsthul, J., Miller, H., 1997. Textures and fabrics in the GRIP project. J. Geophys. Res. 102 (C12), 26583–26599.

Vinther, B.M., Clausen, H.B., Johnsen, S.J., Rasmussen, S.O., Andersen, K.K., Buchardt, S.L., Dahl-Jensen, D., Seierstad, I.K., Siggaard-Andersen, M.L., Steffensen, J.P., Svensson, A.M., Olsen, J., Heinemeier, J., 2006. A synchronized dating of three greenland ice cores throughout the Holocene. J. Geophys Res 111 (D13102).

Wang, Y., Azuma, N., 1999. A new automatic ice-fabric analyzer which uses image-analysis techniques. Ann. Glaciol. 29, 155–162.

Wilen, L.A., Diprinzio, C.L., Alley, R.B., Azuma, N., 2003. Development, principles, and, applications of automated ice fabric analysers. Microsc. Res. Tech. 62, 2–18.